A 3.1-10.6 GHz Ultra-Wideband Pulse-Shaping Mixer

David D. Wentzloff, Anantha P. Chandrakasan

Microsystems Technology Laboratories, Massachusetts Institute of Technology,
Cambridge, MA, 02139, USA, email: ddw@mit.edu

***Abstract* — This paper presents a mixer for pulse-based ultra-wideband (UWB) communication. Pulses are shaped using a new technique that accurately approximates a Gaussian pulse by exploiting the properties of a BJT. The mixer is fabricated in a 0.18µm SiGe BiCMOS process. Simulation and experimental results are presented.**

***Index Terms* — Pulse generation, radio frequency integrated circuits, transmitters, ultra-wideband, UWB.**

I. Introduction

This paper presents a mixer for ultra-wideband (UWB) communication fabricated in a 0.18µm SiGe BiCMOS process that uses a new tanh shaping technique to generate approximate Gaussian pulses in the 3.1-10.6 GHz band. The shape of the transmitted pulse directly determines the -10 dB bandwidth of the signal, specified by the FCC to be at least 500 MHz for UWB. The Gaussian pulse is desirable because it has no side lobes and a sharp roll-off relative to other passive filtered pulses. The Gaussian pulse cannot be generated with passive components alone since it is an exponential shape, and digital filtering implies pulse synthesis which is power hungry at UWB bandwidths. Previous work has shown that pulse generation is performed by direct synthesis, step recovery diodes [1], cascaded filters [2], or other approximations [3], [4].

This paper describes a simple pulse generator with hyperbolic tangent shaping that approximates a Gaussian pulse, up-converts pulses to the 3.1-10.6 GHz band with a near-Gaussian spectrum, and demonstrates matched positive and negative pulses. Simulation and experimental results are provided for the packaged chip.

II. UWB Architecture

The MIT UWB architecture uses pulse-based, binary phase-shift keyed (BPSK) communication where information is encoded as a pulse with either positive or negative polarity [5]. The pulse repetition frequency (PRF) is 100 MHz. A baseband pulse train is up-converted to one of 14 non-overlapping channels in the 3.1-10.6 GHz UWB band. The receiver down-converts the signal to baseband where is it digitized with a 5-bit ADC. During acquisition, the digital back-end learns the pulse shape for only one polarity pulse. Under the assumption that positive and negative pulses are equal and opposite, the back-end uses the learned pulse and its inverse when correlating a BPSK signal. For this reason, amplitude and timing matching between positive and negative transmitted pulses are critical to the quality of service. The linearity requirement in the transmitter is relaxed since the pulse shape is learned before demodulation.

III. Tanh Pulse Shaping

The goal of this work was to design a low-power UWB transmitter that emits Gaussian shaped pulses due to their desirable frequency response. The authors found that by exploiting the exponential behavior of a BJT, the Gaussian pulse can be accurately approximated with an elegant analog circuit that simultaneously performs up-conversion mixing.

A. Circuit Operation

The transmitter uses a differential pair with a triangle signal input to generate and shape a pulse of one polarity, shown conceptually in Fig. 1. For the proper choice of the normalized parameters A, PW, and V_{off} of the input signal, the current i_{C2} will have a shape that approximates that of a Gaussian.

For a fixed bias current I_B, the collector currents in the differential pair are approximately related by

$$I_B = i_{C1} + i_{C2}$$

By substituting terms into the exponential equations for collector current of a BJT, it is easy to show using hyperbolic identities that the collector current i_{C2} is

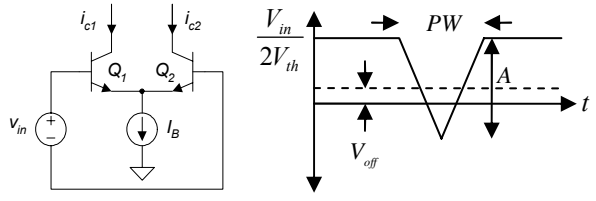

Fig. 1. BJT differential pair and input voltage waveform for generating a tanh pulse.

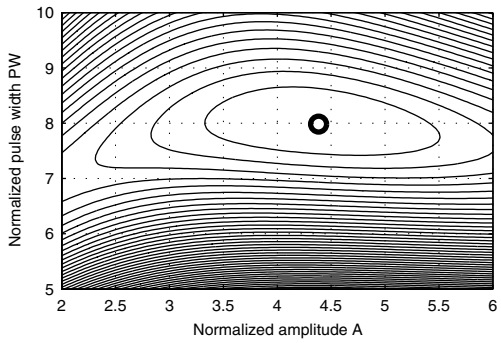

Fig. 2. Mean squared error contours and minimum error point for = 1, V_{off} = 1.0.

described by

$$i_{C2} = \tfrac{1}{2} I_B \left[1 - \tanh\left(V_{in}/2V_{th}\right)\right]$$

The output current i_{C2} of the differential pair will be a pulse with tanh shaped rising and falling edges for the triangle input signal shown in Fig. 1. Note that the *y*-axis is normalized to $V_{in}/2V_{th}$, the argument of the tanh function in the above equation. Current i_{C1} is not used, and can be terminated to the power supply.

This architecture has several benefits: 1) The input signal begins and ends at the same level; thus, there is no "reset" phase required as in differentiating pulse generators, eliminating transients. 2) Positive and negative pulses are generated with the same triangle input signal for better pulse matching, which is difficult to achieve with complementary circuits. 3) Up-conversion is performed by adding an RF signal to the tail current I_B; thus, no additional mixer is required. 4) The triangle signal is generated with well-known techniques, and the accuracy of the Gaussian approximation is not sensitive to small deviations in the values of *A* and *PW*.

B. Optimization

The optimal values for *A*, *PW*, and V_{off} were found empirically by sweeping each variable and finding the minimum mean squared error (MSE) between the resulting tanh-shaped pulse and a Gaussian pulse

$$V_{Gauss} = V_p e^{-t^2/2\sigma^2} .$$

The energies of the two pulses are equalized before calculating the MSE. A contour plot of the MSE vs. *A* and *PW* is shown in Fig. 2 for V_{off} = 1.0 and = 1.0. The minimum MSE point is indicated by the circle, and the corresponding pulse for these values is shown in Fig. 3. As shown in Fig. 2, the minimum MSE between the tanh and Gaussian pulses is broad. This relaxes the requirements on the circuitry needed to generate the

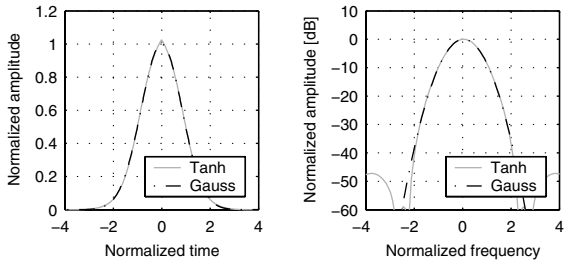

Fig. 3. Time and frequency response of the optimized tanh pulse for = 1, and V_{off} = 1.0.

triangle signal. Equations for determining the optimum values given are summarized below:

1) Normalized Amplitude *A* – The amplitude does not vary with , and varies linearly with V_{off} for $V_{off} > 1.0$. The equation for setting *A* is

$$A = 2.4 + 2.0 \cdot V_{off}$$

2) Pulse Width *PW* – The pulse width is proportional to , and varies linearly with V_{off} for $V_{off} > 1.0$. The equation for setting *PW* is

$$PW = \sigma\left(4.37 + 3.61 \cdot V_{off}\right)$$

3) Normalized offset V_{off} – The normalized offset does not vary with , and should be greater than 1.0 for best results. Making it arbitrarily large does not improve the response.

$$V_{off} \geq 1.0$$

IV. TANH TRANSMITTER

A block diagram of the complete transmitter is shown in Fig. 4. The triangle input signal is implemented off-chip. To generate BPSK pulses, the triangle signal is switched to either the positive or negative input of the mixer. The inactive input is simultaneously switched to a constant voltage. The same triangle signal is used to generate both polarity pulses to improve matching. The triangle signal switch also has an off state to implement a variable PRF or standby mode. The up-converted pulse is filtered and amplified on-chip before being sent to the off-chip UWB antenna.

A schematic of the tanh pulse-shaping mixer is shown in Fig. 5. The local oscillator (LO) signal can be switched between an on-chip voltage controlled oscillator (VCO) and an external LO input. The LO signal path is balanced for equal amplitudes and 180° phase difference between the differential signals. The differential LO signal is converted to a current and mirrored, along with a bias current, into the tails of the two differential pairs.

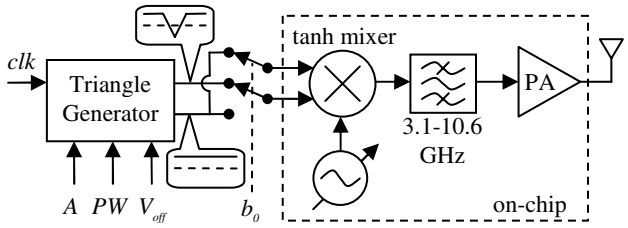

Fig. 4. BPSK UWB transmitter block diagram.

Up-converted positive or negative pulses are generated by applying the triangle input signal to V_{in+} or V_{in-}, respectively. The triangle signal voltage is relative to V_{cm}, which is at a fixed potential. Applying the triangle signal to $Q_{3+/-}$ with the bases of $Q_{4+/-}$ fixed reduces the coupling between the mixer inputs and the output. The output currents of the differential pairs are summed at node V_{out}. This provides first-order cancellation of LO feedthrough, similar to a double-balanced Gilbert cell mixer.

A schematic of the UWB band select filter and power amplifier (PA) is shown in Fig. 6. The mixer output is fed into the filter made by L_1, L_2, and C_1, providing a 2nd-order roll-off below 3 GHz to reduce out-of-band emissions. The signal is then buffered and AC coupled to the PA. The PA is class A, with an RF choke at the output, and can be DC coupled to the antenna.

V. Simulation Results

The transmitter was simulated with parasitic resistances and capacitances extracted from the layout. Matching between positive and negative pulses, LO feedthrough, and the frequency response were evaluated. Simulation results indicate excellent matching between pulses when using the on-chip VCO. Simulations for LO feedthrough predict a maximum of -49 dBm at 3 GHz dropping to -56 dBm at 10 GHz, well below the -41.3 dBm FCC limit. The simulated frequency response is shown in Fig. 7. This figure plots the peak amplitude of an up-converted pulse at each of the 14 channel center frequencies. The center frequencies are set by

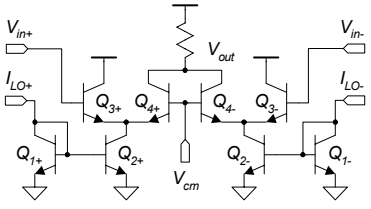

Fig. 5. Schematic of the tanh pulse shaping UWB mixer.

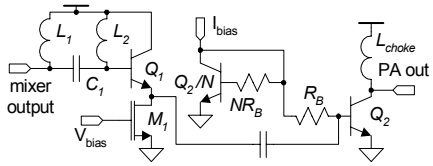

Fig. 6. Schematic of the filter and power amplifier.

$$f_{center} = 2904 + 528 \cdot n_{ch} \ [MHz]$$

where n_{ch} = 1, 2, …, 14. The simulated power of the pulse in the highest channel is roughly 5dB lower than that of the mid-band channels.

VI. Experimental Results

The transmitter was fabricated in a 0.18µm SiGe BiCMOS process. A die photo is shown in Fig. 8. The chip was packaged in a 48 lead QFN package; a wirebonded package that limited the performance at high frequencies. The total DC power consumption of the PA, mixer, and LO buffering was 31.3 mW.

A. Up-Converted Pulse Response

When provided the triangle input signal described in Section III, the transmitter generates a pulse 2ns wide with a spectrum centered around the LO frequency. The -10dB bandwidth of the pulse is 500 MHz. One such measured pulse is shown in Fig. 9. This signal has been up-converted to a center frequency of 4.0 GHz using an external LO locked to the PRF, and has a peak amplitude of 130 mV.

B. Steady State Matching

The steady-state RF output power was measured while sweeping the input voltage to the differential pairs at the positive and negative pulse inputs to the mixer. This

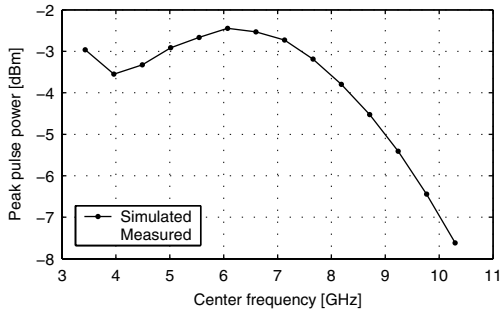

Fig. 7. Simulated frequency response for pulses up-converted to 14 different center frequencies.

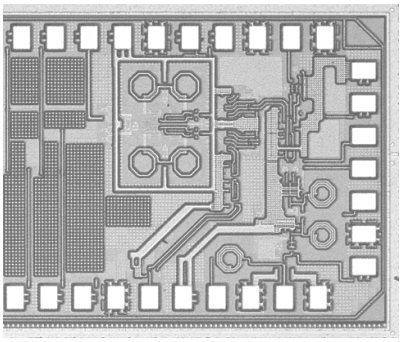

Fig. 8. Die photo of the UWB transmitter.

measures the matching in steady-state response between positive and negative pulses, LO feedthrough, maximum power, and offsets. The results are shown in Fig. 10, using the on-chip VCO for the best matching. The results are compared to an ideal tanh response (in light gray). Mismatch causes the discrepancy between the measured and ideal tanh response, which is 0 for a 0.1 V input due to perfect LO cancellation. The positive and negative results show excellent matching within the precision of the measurement, and generally follow the tanh response.

VII. Conclusions

A new technique for generating pulses that accurately approximates a Gaussian shape is presented. By exploiting the exponential properties of a BJT, a near-Gaussian pulse is shaped from a triangle input signal. Pulse shaping is integrated into the mixer, performing up-conversion and shaping in one simple circuit. The measured frequency response is limited due to packaging; however, matched positive and negative pulses, and near-Gaussian pulse generation has been demonstrated.

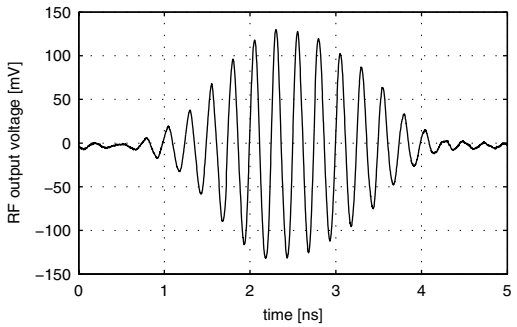

Fig. 9. Measured tanh shaped pulse modulated by a 4.0 GHz external LO.

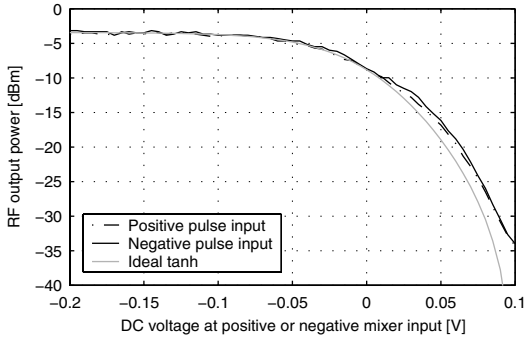

Fig. 10. Measured output power at 3.3 GHz for a swept DC voltage applied to the positive and negative mixer inputs.

Acknowledgements

This material is based upon work supported by the National Science Foundation under Grant No. ANI-0335256. Any opinions, findings, and conclusions or recommendations expressed in this material are those of the authors and do not necessarily reflect the views of the National Science Foundation. This research is also sponsored by the HP-MIT Alliance.

References

[1] J. Han, C. Nguyen, "Ultra-Wideband Electronically tunable Pulse Generators," *IEEE Microwave and Wireless Components Letters*, Vol. 14, No. 3, March 2004, pp 112-114.

[2] S. Baggat, et al, "A PPM Gaussian Monocycle Transmitter for Ultra-Wideband Communications," *International Workshop on UWB Systems*, May 2004.

[3] A. Azakkour, et al, "Challenges for a new integrated Ultra-wideband (UWB) source," *IEEE Conference on UWB Systems and Technologies*, November 2003.

[4] H. Kim, et al, "Design of CMOS Scholtz's Monocycle Pulse Generator," *IEEE Conference on UWB Systems and Technologies*, November 2003.

[5] R. Blazquez, et al, "A Baseband Processor for Pulsed Ultra-Wideband Signals," *IEEE Custom Integrated Circuits Conference*, October 2004.